Title

Establishment and characterization of two novel patient-derived lines from canine high-grade glioma.

Journal

Veterinary and Comparative Oncology, 21(3)

Authors

Schrock, Morgan

Zalenski, Abigail

Tallman, Miranda

et al.

Publication Date

2023-09-01

DOI

10.1111/vco.12912

Peer reviewed

HHS Public Access

Author manuscript

Vet Comp Oncol. Author manuscript; available in PMC 2024 September 01.

Published in final edited form as:

Vet Comp Oncol. 2023 September ; 21(3): 492–502. doi:10.1111/vco.12912.

Establishment and characterization of two novel patient-derived lines from canine high-grade glioma

Morgan S Schrock[1,*], **Abigail A Zalenski**[1,2], **Miranda M Tallman**[1,3], **Luke Kollin**[1], **Anna Bratasz**[4], **Griffin Weeks**[4], **Margaret A Miller**[5], **Courtney N Sweeney**[5], **G Elizabeth Pluhar**[6], **Michael R Olin**[7], **William C. Kisseberth**[8], **R Timothy Bentley**[9], **Peter J Dickinson**[10], **Daniel York**[10], **Amy Webb**[11], **Xu Wang**[12], **Sarah Moore**[8], **Monica Venere**[1], **Matthew K Summers**[1,*]

[1]Department of Radiation Oncology, Arthur G James Comprehensive Cancer Center and Richard L. Solove Research Institute, The Ohio State University, Columbus, OH, USA

[2]Neuroscience Graduate Program, The Ohio State University, Columbus, OH, USA

[3]Biomedical Sciences Graduate, Program The Ohio State University Columbus, OH, USA

[4]Small Animal Imaging Core, The Ohio State University, Columbus, OH, USA

[5]Department of Comparative Pathobiology, Purdue University, West Lafayette, IN, USA

[6]Department of Veterinary Clinical Sciences, College of Veterinary Medicine, University of Minnesota, St Paul, Minnesota, USA

[7]Department of Pediatrics, Division of Pediatric Hematology and Oncology, Masonic Cancer Center, University of Minnesota, Minneapolis, MN, USA

[8]Department of Veterinary Clinical Sciences, The Ohio State University, Columbus, OH, USA

[9]Department of Veterinary Clinical Sciences, Purdue University, West Lafayette, IN, USA

[10]Department of Surgical and Radiological Sciences, UC Davis School of Veterinary Medicine, The University of California, Davis, CA, USA

[11]Department of Biomedical Informatics, The Ohio State University, Columbus, OH, USA

[12]Department of Pathobiology, Auburn University, Auburn, AL, USA.

Abstract

High-grade glioma is an aggressive cancer that occurs naturally in pet dogs. Canine high-grade glioma (cHGG) is treated with radiation, chemotherapy or surgery, but has no curative treatment. Within the past eight years, there have been advances in our imaging and histopathology standards as well as genetic charactereization of cHGG. However, there are only three cHGG cell lines publicly available, all of which were derived from astrocytoma and established using methods involving expansion of tumor cells *in vitro* on plastic dishes. In order to provide more clinically relevant cell lines for studying cHGG *in vitro*, the goal of this study was to establish

[*]Lead contact; Correspondence: Matthew K Summers, matthew.summers@osumc.edu and Morgan S Schrock moschrock@gmail.com.

Conflict of Interest

The authors declare that the research was conducted in the absence of any commercial or financial relationships that could be construed as a potential conflict of interest.

cHGG patient-derived lines, whereby cancer cells are expanded *in vivo* by injecting cells into immunocompromized laboratory mice. The cells are then harvested from mice and used for *in vitro* studies. This method is the standard in the human field and has been shown to minimize the acquisition of genetic alterations and gene expression changes from the original tumor. Through a multi-institutional collaboration, we describe our methods for establishing two novel cHGG patient-derived lines, Boo-HA and Mo-HO, from a high-grade astrocytoma and a high-grade oligodendroglioma, respectively. We compare our novel lines to G06-A, J3T-Bg, and SDT-3G (traditional cHGG cell lines) in terms of proliferation and sensitivity to radiation. We also perform whole genome sequencing and identify an NF1 truncating mutation in Mo-HO. We report the characterization and availability of these novel patient-derived lines for use by the veterinary community.

Keywords

Canine high-grade glioma; Canine oligodendroglioma; Patient-derived line; Canine brain cancer; Radiation

Introduction

High-grade glioma is an aggressive cancer in pet dogs for which there is no standard of care. Options for treatment include surgery and radiation with varying impact on overall survival[1–2]. Within the past eight years there have been significant advances in our guidelines on diagnostic imaging, histopathological diagnosis as well as genetic and epigenetic characterization of cHGG[3–5]. However, there remains a lack of cHGG cell lines for testing novel therapies *in vitro*. There are currently only four canine glioma cell lines described in the literature, all of which are astrocytoma, and one of which is no longer available[6–8]. In addition, these cell lines were established using traditional methods, whereby tumors are minced and cultured on plastic dishes in medium supplemented with fetal bovine serum. Because recent work in human high-grade glioma revealed significant genetic and gene expression changes in traditionally established cell lines compared to primary tumors, the standard in the human field has shifted away from using cell lines to using patient-derived lines for *in vitro* work[9–12]. Instead of expanding cancer cells *in vitro*, patient-derived lines require cancer cells to be expanded *in vivo* by injecting cells heterotopically (subcutaneously) or orthotopically (intracranially) into immunocompromized laboratory mice[12]. The cells are thus allowed to grow in an *in vivo* environment and are harvested when mice exhibit symptoms of tumor burden, then used for *in vitro* studies. Another key difference is that patient-derived lines are cultured in medium where fetal bovine serum (FBS), a supplement common in medium for traditional cell lines, is replaced with basic Fibroblast Growth Factor (bFGF) and Epidermal Growth Factor (EGF). This replacement is due to a landmark study in 2006 which revealed that primary glioma cells grown in FBS lost the presence of tumor stem cells and exhibited significant genetic and biologic differences from the parental tumor cells[13]. In contrast, tumor cells grown in medium supplemented with bFGF and EGF retained the presence of tumor stem cells and recapitulated the genotype, biology, and gene expression profile of the primary tumors[13].

Despite the advances in our understanding and classification of cHGG, there remains a need for clinically relevant patient-derived lines of cHGG. Thereofre, the goal of this study was to establish novel cHGG lines to encompass all types of glioma (including oligodendroglioma) in a manner that best recapitulates original tumor genetics using patient-derived lines[14]. Herein we report our methods and characterization of two novel patient-derived lines, Boo-HA and Mo-HO, derived from high-grade astrocytoma and high-grade oligodendroglioma, respectively.

Methods

Cells and culture conditions

All cells were cultured at 37°C at 5% CO_2. Mo-HO and Boo-HA cells were cultured as described previously using Neural Stem Cell (NSC) medium on plates pre-treated with Geltrex (Thermo Fisher) and passaged using TrypLE Express Enzyme (no phenol red; Gibco)[15]. G06-A, J3T-Bg, SDT-3G cells were cultured as described and passaged with 0.25% Trypsin (Sigma)[6,7]. See Supplemental Text for expanded methods.

Cell Line Validation Statement

All canine cell lines G06-A, J3T-Bg, SDT-3G, Mo-HO, Boo-HA) were validated as unique, uncontaminated lines of canine origin with polymorphic short tandem repeat loci (STR) by Cell Line Services.

Tissue procurement and pathological analysis

All tumor tissues acquired intraoperatively from pet dogs undergoing therapeutic resection were obtained following informed consent in compliance with guidelines outlined by the Veterinary Clinical Trials Office (Purdue University, University of Minnesota). The histopathological analysis occurred at the corresponding institution immediately after surgery by a board-certified veterinary pathologist to confirm diagnosis and inform treatment plan. For analysis, tissue fragments from the formalin-fixed surgical biopsy specimen were embedded en masse in paraffin for routine histologic processing. Diagnosis was based on evaluation of hematoxylin and eosin (HE)-stained sections with immunohistochemistry for Olig2, glial fibrillary acidic protein (GFAP), IBA1, vimentin, and/or synaptophysin. Glioma grading was based on CBTC criteria for Mo-HO but not Boo-HA since that sample predates the updated guidelines[4].

Tumor tissue processing

For fresh samples, tissue was sent from the veterinary neurosurgeon overnight on ice in tissue culture medium to the collaborating laboratory where it was immediately processed with papain digestion and red blood cell lysis (Papain Dissociation System; Worthington Biochemical)[15]. Cell number was quantified using trypan blue stain and the standard operating protocol (Figure 2a) was consulted to determine number of cells and injection location into mice. Cells were implanted into mice as previously described on the same day of processing[15]. Samples (n=10) which had been processed and frozen at low passage (<4) from the University of Minnesota were shipped overnight on dry ice as cryopreserved aliquots, then revived and grown as described above until sufficient cells were present for

injections[16]. For harvesting tumor tissue from laboratory mice, the Papain Dissociation System was used again with the addition of a follow-up step to ensure depletion of mouse cells in canine tumor samples using magnetic bead -based sorting (Miltenyi Biotec). See Supplemental Text for expanded methods.

Laboratory animals and *in vivo* studies

All experiments using laboratory mice to expand cHGG cells were approved by OSU Institutional Animal Care and Use Committee (IACUC) and were conducted in accordance with the NIH Guide for the Care and Use of Laboratory Animals. Male athymic nude Nu/Nu mice were obtained from the Nu/Nu colony managed by the OSU Comprehensive Cancer Center Target Validation Shared Resource. SC and IC injections were performed as described previously, but following our own standard operating protocol (Figure 2a) to inform location and number of cells to inject[15]. See Supplemental Text for expanded methods.

Monitoring cHGG cell growth in laboratory mice

cHGG cells injected SC were monitored with digital caliper measurements twice weekly. Cells orthotopically injected IC were monitored every 1–3 months with microMRI imaging (BioSpec 94/30USR Imaging System Bruker BioSpin Co.) under general anesthesia with a protocol approved by OSU IACUC. See Supplemental Text for expanded methods.

In vitro cell growth assays via live cell imaging

To encourage adherence and growth of Boo-HA and Mo-HO cells as a monolayer instead of neurospheres, 96-well plates were pre-treated with Gel-trex when seeding those lines, whereas wells for G06-A, J3T-BG, SDT-3G remained untreated as is the norm for those cell lines. The day after seeding, cells were irradiated with 2 Gy or 4 Gy using a GammaCell 40 Irradiator (Best Theratronics). Plates were then placed in the IncuCyte ZOOM live cell imaging system (Sartorius) with phase-contrast images taken every 4 hours for 6 days. Resulting images were analyzed using the IncuCyte ZOOM analysis software for label-free proliferation measurements using optimized processing definitions, which track confluence over time.

Long-term growth assays

Six-well plates were pre-treated with Gel Trex (Boo-HA, Mo-HO) or left untreated (Go6A, J3T-BG, SDT 3G) then seeded with 250 cells. Cells were irradiated as above. Media was changed one day later, then fixed with methanol ten days post-treatment and stained with 0.5% crystal violet solution. Plates were imaged and analyzed using LI-COR Odyssey near infrared imaging system to quantify intensity per well.

Whole genome sequencing library preparation

Mo-HO and Boo-HA cells were grown to ~70% confluence, then DNA was isolated using DNeasy Blood and Tissue Kit (QIAGEN). DNA concentrations were measured by a Qubit 3.0 Fluorometer (Thermo Fisher Scientific) and A260/A280 absorption ratios were measured on a NanoDrop OneC Spectrophotometer (Thermo Fisher Scientific). A total of

1.μg genome DNA was fragmented by M220 Focused-ultrasonicator for a 550bp targeted insert size (Covaris). DNA sequencing libraries were constructed using NEBNext Ultra II DNA Library Prep Kit for Illumina (New England Biolabs). The final library concentration was accessed with Qubit 3.0 Fluorometer, and the size distribution was checked on a Perkin-Elmer LabChip GX Touch HT machine (PerkinElmer, MA). After QC, the libraries were sequenced on an Illumina NovaSeq6000 sequencer using 150 bp paired-end configuration. Genome sequencing data is available at NCBI SRA (Short Read Archive) under accession number PRJNA957755. For variant analysis methods see Supplemental Text.

Statistical Methods

For *in vitro* proliferation and radiation sensitivity graphs (Figure 4a, Figure 5, Figure 6b), each experiment was repeated three times per line with three technical replicates per repeat. Data were analyzed via a 2-way ANOVA with a Tukey's post-hoc multiple comparison test and significance at endpoint is shown. Error bars represent standard error; ns, no significance; *, $p < 0.05$; ***, $p < 0.001$; ****, $p < 0.0001$.

Results

Workflow and acquisition of cHGG samples

We created a workflow (Figure 1) that enabled us to link expertise across multiple academic centers to establish patient-derived lines of cHGG. We obtained two types of cHGG samples from collaborators: fresh tissue obtained intraoperatively (n=2) and frozen cells minimally processed and at very low passage (n=10). Fresh samples were shipped overnight in sterile tissue culture media and processed with a papain digestion and red blood cell lysis upon receipt, then counted and injected IC into athymic nude mice. In contrast, frozen cHGG cells were not processed, but were cultured *in vitro* for one or two passages to sufficiently expand cell number for injecting IC into mice (100,000 cells). With both fresh and frozen cHGG cells, a standard operating protocol (SOP) was consulted to determine the workflow for number of cells and route of injections (Figure 2a). This SOP placed a priority on orthotopic engraftment of tumor cells rather than heterotopic due to retention of the original tumor microenvironment and >50% reported engraftment rates[12,17].

Both fresh tissue samples were high-grade oligodendroglioma. Due to low cell number after processing, the first sample was injected SC into mice and did not show signs of tumor after 12 months, therefore the mouse was euthanized. Histopathological assessment of the tumor from the second sample revealed histologic sections composed exclusively of densely cellular and well-vascularized neoplastic tissue with multifocal hemorrhage (Figure 2b). The neoplastic cells were polygonal to fusiform with a large round to oval nucleus, variable chromatin content and nuclear diameter, 1–2 distinct nucleoli, 6 mitotic figures in 2.37 mm^2, and scanty to moderate amount of pale wispy eosinophilic cytoplasm with faint cell borders. In a few fields, the neoplastic cells were rounder with a round nucleus and artifactual perinuclear clearing, resulting in the classic honeycomb pattern (Figure 2c). The initial diagnosis was high-grade glioma. Immunohistochemically, the neoplastic cells were positive for Olig2, consistent with oligodendrocyte origin, and negative for GFAP and IBA1, ruling out astrocytoma and histiocytic sarcoma, respectively, so the diagnosis was refined to

high-grade oligodendroglioma. After processing in the laboratory, this sample had sufficient cells to engraft IC and SC into mice. We maintained a naming system that used the first syllable of the patient name followed by HO for high-grade oligodendroglioma diagnosis or HA for high-grade astrocytoma diagnosis, therefore this sample was named Mo-HO.

We received ten cHGG samples (5 oligodendroglioma and 5 astroctyoma) from the University of Minnesota that were stored as frozen cells in liquid nitrogen. Unfortunately, we were only able to expand one sample, Boo-HA, sufficiently *in vitro* to inject IC into mice. We believe the age of the cells (some of which were ten years old), differences in basement membrane used (Matrigel was used at University of Minnesota to initially expand the cells, GelTrex was used at OSU), and the fact that not all primary tumor cells expand sufficiently in an *in vitro* setting were all factors that contributed to only the Boo-HA sample expanding sufficiently. The histopathological analysis of this sample after surgery revealed that microscopically, the neoplastic cells were polygonal to elongate with discrete cell borders, small amounts of fibrillary cytoplasm, polygonal nuclei, hyperchromatic to vesicular chromatin and indistinct nucleoli. Immunohistochemically, the tumor was negative for vimentin and synaptophysin, but positive for GFAP (60%). Histomorphologically the tumor had several features characteristic of a fibrillary astrocytoma, a histologic variant of astrocytoma, so the final diagnosis was high-grade astrocytoma.

Monitoring cHGG cells in laboratory mice

In order to monitor growth of cHGG cells injected IC into mice, we performed routine microMRI imaging (Figure 3). Because of the high number of cells present after processing from the Mo-HO sample, we were able to inject two mice IC (one mouse with 100,000 cells and one mouse with 20,000 cells) and three mice SC with unprocessed tissue pieces. As evident from the scans (Figure 3a), Mouse 1 injected with 100,000 Mo-HO cells had a normal microMRI scan 12 weeks after injections, but by 16 weeks there was a sizeable mass with brain structure deformation and a hyperintense region (arrow) that became more progressive with dramatic midline shift in the last scan taken at 20 weeks. Mouse 1 was sacrificed at 21 weeks (Figure 3b) and cells were harvested and processed again as outlined in Figure 1 and the expanded methods (Supplemental Text). Mouse 2 was injected with 20,000 Mo-HO cells and microMRI imaging at 20 weeks revealed a hyperintense region (arrow). By 38 weeks, the scan revealed brain asymmetry with significant midline shift that progressed in the last scan (46 weeks). This mouse was sacrificed 48 weeks post IC injection, compared to 21 weeks when five times the number of cells were injected (Mouse 1). This 27-week difference in incubation time between Mouse 1 (injected with 100,000 cells) compared to Mouse 2 (injected with 20,000 cells) highlights the importance of injecting a large cell number when possible.

Three mice were also engrafted with unprocessed Mo-HO tissue pieces SC. Tumor growth was monitored weekly with digital caliper measurements with a variability of tumor growth, including one mouse (Mouse 5) which did not show engraftment of Mo-HO cells by 46 weeks and was therefore sacrificed (Figure 3b).

Mouse 6 was injected with 100,000 Boo-HA cells IC. MicroMRI imaging at 15 weeks revealed a hypointense region which was significantly larger in the 23-week scan, with

midline deviation and an apparent secondary mass in the left hemisphere. Mouse 6 was sacrificed after the last scan at 23 weeks and the cells were harvested. Noteworthy is the fact that Mouse 7, which was injected with five times fewer Boo-HA cells than Mouse 6, was sacrificed only 2 weeks afterwards- highlighting the importance of routine scanning and daily monitoring for early removal criteria in these mice.

Growth of Mo-HO and Boo-HA patient-derived lines *in vitro*

In order to ensure that cHGG cells cultured following IC or SC growth in laboratory mice did not contain mouse cell infiltrates, we performed magnetic bead-based sorting of harvested cells using a mouse cell depletion kit. As a second check that we had successfully isolated a pure population of canine cells, we fixed harvested cells before and after mouse cell depletion then stained with DAPI to quantify the percentage of canine cells compared to mouse cells (Supplemental Figure 1a, 1b). This analysis takes advantage of morphological differences of DAPI staining in mouse cells[18]. We confirmed tumorigenicity of Mo-HO and Boo-HA cells at xenograft passage xp1 (after harvesting from mice) by re-injecting IC into mice.

In order to assess the growth of our newly established patient derived lines, we sought to compare them to the canine SDT-3G, G06-A, (both high-grade astrocytoma) and J3T-Bg (anaplastic astrocytoma) cell lines which are commonly used by the veterinary community[16,19,20]. We assessed *in vitro* cell growth using the IncuCyte live cell imaging system to capture images of cells over time and calculate growth as a measure of confluence, normalized to the first time point (Figure 4a and Supplemental Figure 1c). The novel patient-derived lines Mo-HO and Boo-HA exhibit the slowest growth, with doubling times of 128 hr and 42 hr respectively, whereas SDT-3G, J3T-Bg and G06-A are faster growing with doubling times of 36 hr, 22 hr and 18 hr, respectively. Photomicrographs of the cell lines reveal a varied morphology (Figure 4b), with the G06-A and J3T-BG cell lines exhibiting clustering at confluences above approximately 50–60%, which can affect proliferation measurements assessed by confluence over longer time courses (Supplemental Figure 1c).

Sensitivity of Mo-HO and Boo-HA lines to radiation

Because radiation is a treatment option for dogs with cHGG, we sought to determine the sensitivity of our novel patient-derived lines to radiation[21–23]. We exposed plated cHGG cells to 0, 2, or 4 Gy of radiation then monitored cell growth with the InucCyte live imaging system (Figure 5). The cHGG lines exhibited variable sensitivities to radiation. The SDT-3G cells were the most sensitive with a relative three-fold decrease in growth over a 72-hour time period, whereas the Mo-HO patient-derived line was the most resistant with a 1.1-fold decrease in growth.

To evaluate long-term cell survival *in vitro*, we plated cells sparsely, exposed them to either 0, 2, or 4 Gy of radiation, then stained after 14 days (Figure 6). All cell lines formed discrete colonies with the exception of the Mo-HO line (Figure 6a). We observed variable sensitivities to radiation (Figure 6b) with G06-A and J3T-Bg being the most sensitive with 42% and 46% survival compared to the more resistant lines, SDT-3G and Boo-HA with 74% and 71% survival, respectively, after exposure to 4 Gy (Figure 6c).

Genetic characterization of Mo-HO and Boo-HA lines

In order to determine genetic alterations responsible for driving tumorigenesis in our Mo-HO and Boo-HA samples, we performed whole genome sequencing and analyzed variants present in 20 genes (shown in Figure 7) most commonly altered in human and canine high-grade glioma[5,24]. Both lines exhibited low-impact variants across the genes (Figure 7 and Supplemental Excel File). However, we identified a high-impact missense variant in NF1 which caused a premature stop in Mo-HO patient-derived line. Interestingly, a recent genetic analysis of 83 cHGG samples found NF1 to be the third most frequently altered gene among a panel of low and high-grade canine oligodendroglioma and astroctyoma samples[5]. Boo-HA patient-derived line featured two moderate-impact missense variants within the ARID5B gene (Supplemental Excel File).

Discussion

cHGG is an aggressive disease with no cure. There are three cell lines available in the literature for studying cHGG in the laboratory, however, these lines are all derived from astrocytoma primary tumors. Within this study we sought to increase the number and types of cHGG lines available by creating patient-derived lines, which require *in vivo* expansion of cancer cells. Patient-derived lines are cultured in tissue culture medium supplemented with growth factors shown to promote the presence of cancer stem-cell like tumor cells[13]. In addition, the medium lacks serum, which has been shown to alter the genome and transcriptome of cancer cells[9].

Herein, we report the establishment and characterization of two novel cHGG patient-derived lines, Mo-HO and Boo-HA. Additionally, we share our workflow and methods (see Supplemental Text for expanded methods) that enabled us to generate these lines using resources across different institutions. At Ohio State University Veterinary Medical Center, our standard of care for treating cHGG is radiation, therefore, our only opportunity to obtain cHGG tissue samples is during necropsy after owner elected euthanasia, and even then, the tissues are presumptive cHGG based on imaging until histopathology can be performed. Although we were not able to obtain samples via necropsy post euthanasia, it is another source of tumor tissue that should continue to be explored to increase the number of cHGG patient-derived lines available. Because our approach was successful with overnight shipping of tumor cells to a lab at another institution, we hope our methods will provide a guide to enable scientists and clinicians with unique expertise across different institutions to establish more cHGG patient-derived lines.

When characterizing the growth and sensitivity to radiation of our novel patient-derived lines, we also included the commonly used cHGG cell lines G06-A, J3T-Bg, and SDT-3G. These cell lines were established using traditional methods in medium containing fetal bovine serum and devoid of growth factors. Because our goal was to provide a comparison for the veterinary community to reference when deciding which cells to use, we cultured G06-A, J3T-Bg, and SDT-3G using the medium in which they were established. Therefore, the differences in medium between patient-derived lines and traditionally established lines may contribute to the differences in cell growth and sensitivity to radiation reported here.

One technical challenge we did encounter in mice being monitored for cHGG cell growth after injection of cells IC was a lack of tumor enhancement post Gd-based contrast imaging (Figure 3). Engrafted cHGG cell growth was evident when tumors were large, mostly due to changes in brain anatomy, such as midline shift. Since our goal with the intracranial injections was to expand the cell number as much as possible, we did not need to detect small tumors so the imaging was sufficient for our studies. However, future work establishing similar lines may benefit from incubating supramagnetic ion oxide (SPIO) particles with cHGG cells prior to IC injection. SPIO particles give a 'negative' contrast in MRI, appearing as hypointense regions on MR images, allowing for more refined monitoring of tumor growth.

In conclusion, we report two novel cHGG patient-derived lines, Boo-HA and Mo-HO, the latter of which is the first published cell line of canine oligodendroglioma. Further study of these two lines will be needed to validate and establish their clinical and translational relevance.

Supplementary Material

Refer to Web version on PubMed Central for supplementary material.

Acknowledgements

This work was supported by OSU College of Veterinary Medicine Canine Research Fund (MSS, SM). Other funding sources included an American Brain Tumor Association Basic Research Fellowship sponsored by an anonymous corporate partner (MSS); NIH R01GM108743 and R01GM112895 (MKS); an American Cancer Society Research Scholars Grant RSG-18-066-01-TBG (MV); NIH 2T32GM068412-11A1 (MMT); an Ohio State University Graduate School Dean's Distinguished University Fellowship (AAZ); the Pelotonia Fellowship Program (MMT and AAZ). Research reported in this publication was supported by the Ohio State University Comprehensive Cancer Center and the National Institutes of Health under grant number P30 CA016058. We thank the Target Validation Shared Resource (OSU Comprehensive Cancer Center) for providing the Nu/Nu mice and the stereotactic instrumentation support. We also thank the Small Animal Imaging Core, supported by NIH 2P30CA016058-45, for GammaCell 40 support, conducting the microMRI scans, and providing consultations. The content is solely the responsibility of the authors and does not necessarily represent the official views of the National Institute of Health.

References

1. Hubbard ME, et al. , Naturally occurring canine glioma as a model for novel therapeutics. Cancer Invest, 2018. 36(8): p. 415–423. [PubMed: 30234401]
2. José-López R, et al. , Clinical features, diagnosis, and survival analysis of dogs with glioma. J Vet Intern Med, 2021. 35(4): p. 1902–1917. [PubMed: 34117807]
3. Packer RA, et al. , Consensus recommendations on standardized magnetic resonance imaging protocols for multicenter canine brain tumor clinical trials. Vet Radiol Ultrasound, 2018. 59(3): p. 261–271. [PubMed: 29522650]
4. Koehler JW, et al. , A revised diagnostic classification of canine glioma: Towards validation of the canine glioma patient as a naturally occurring preclinical model for human glioma. J Neuropathol Exp Neurol, 2018. 77(11): p. 1039–1054 [PubMed: 30239918]
5. Amin SB, et al. , Comparative molecular life history of spontaneous canine and human gliomas. Cancer Cell, 2020. 37(2): p. 243–257.e7. [PubMed: 32049048]
6. Berens ME, et al. , Tumorigenic, invasive, karyotypic, and immunocytochemical characteristics of clonal cell lines derived from a spontaneous canine anaplastic astrocytoma. In Vitro Cell Dev Biol Anim, 1993. 29a(4): p. 310–8. [PubMed: 8320182]

7. York D, et al. , TP53 mutations in canine brain tumors. Vet Pathol, 2012. 49(5): p. 796–801. [PubMed: 22002975]
8. Empl MT, et al. , The growth of the canine glioblastoma cell line D-GBM and the canine histiocytic sarcoma cell line DH82 is inhibited by the resveratrol oligomers hopeaphenol and r2-viniferin. Vet Comp Oncol, 2014. 12(2): p. 149–59. [PubMed: 22882564]
9. Li A, et al. , Genomic changes and gene expression profiles reveal that established glioma cell lines are poorly representative of primary human gliomas. Mol Cancer Res, 2008. 6(1): p. 21–30. [PubMed: 18184972]
10. Xie Y, et al. , The human glioblastoma cell culture resource: Validated cell models representing all molecular subtypes. EBioMedicine, 2015. 2(10): p. 1351–63. [PubMed: 26629530]
11. Liu P, et al. , Preclinical models of glioblastoma: limitations of current models and the promise of new developments. Expert Rev Mol Med, 2021. 23: p. e20. [PubMed: 34852856]
12. da Hora CC, et al. , Patient-derived glioma models: From patients to dish to animals. Cells, 2019. 8(10).
13. Lee J, et al. , Tumor stem cells derived from glioblastomas cultured in bFGF and EGF more closely mirror the phenotype and genotype of primary tumors than do serum-cultured cell lines. Cancer Cell, 2006. 9(5): p. 391–403. [PubMed: 16697959]
14. Woo XY, et al. , Conservation of copy number profiles during engraftment and passaging of patient-derived cancer xenografts. Nat Gen, 2021. 53(1): p. 86–99.
15. Tallman MM, et al. , The small molecule drug CBL0137 increases the level of DNA damage and the efficacy of radiotherapy for glioblastoma. Cancer Lett, 2021. 499: p. 232–242. [PubMed: 33253788]
16. Lai SR, et al. , In vitro anti-tubulin effects of mebendazole and fenbendazole on canine glioma cells. Vet Comp Oncol, 2017. 15(4): p. 1445–1454. [PubMed: 28078780]
17. Kerstetter-Fogle AE, et al. , Generation of glioblastoma patient-derived intracranial xenografts for preclinical studies. Int J Mol Sci, 2020. 21(14).
18. Wang Y, et al. , A convenient method for distinguishing human and mouse cells in situ. Acta Biochim Biophys Sin (Shanghai), 2021. 53(1): p. 124–127. [PubMed: 33206157]
19. Koehler J, et al. , Differential expression of miRNAs in hypoxia (“HypoxamiRs”) in three canine high-grade glioma cell lines. Front Vet Sci, 2020. 7: p. 104. [PubMed: 32258065]
20. Noguchi S, et al. , The NRG3/ERBB4 signaling cascade as a novel therapeutic target for canine glioma. Exp Cell Res, 2021. 400(2): p. 112504. [PubMed: 33508276]
21. Miller AD, Miller CR, and Rossmeisl JH, Canine primary intracranial cancer: A clinicopathologic and comparative review of glioma, meningioma, and choroid plexus tumors. Front Oncol, 2019. 9: p. 1151. [PubMed: 31788444]
22. MAGALHÃES TR, et al. , Outcome after radiation therapy in canine intracranial meningiomas or gliomas. In Vivo, 2021. 35(2): p. 1117–1123. [PubMed: 33622909]
23. Debreuque M, et al. , Definitive-intent uniform megavoltage fractioned radiotherapy protocol for presumed canine intracranial gliomas: retrospective analysis of survival and prognostic factors in 38 cases (2013–2019). BMC Vet Res, 2020. 16(1): p. 412. [PubMed: 33129320]
24. Louis DN, et al. , The 2021 WHO classification of tumors of the central nervous system: A summary. Neuro Oncol, 2021. 23(8): p. 1231–1251. [PubMed: 34185076]

Cell Line Validation Statement

Mycoplasma testing was performed quarterly (LookOut Mycoplasma PCR Detection Kit; Sigma Aldrich) on all four lines. G06-A, J3T-Bg, and SDT-3G lines were a gift of Dr. Peter Dickinson. All canine cell lines described within this manuscript (G06-A, J3T-Bg, SDT-3G, Mo-HO, Boo-HA) were validated as unique, uncontaminated lines of canine origin with polymorphic short tandem repeat loci (STR) by Cell Line Services.

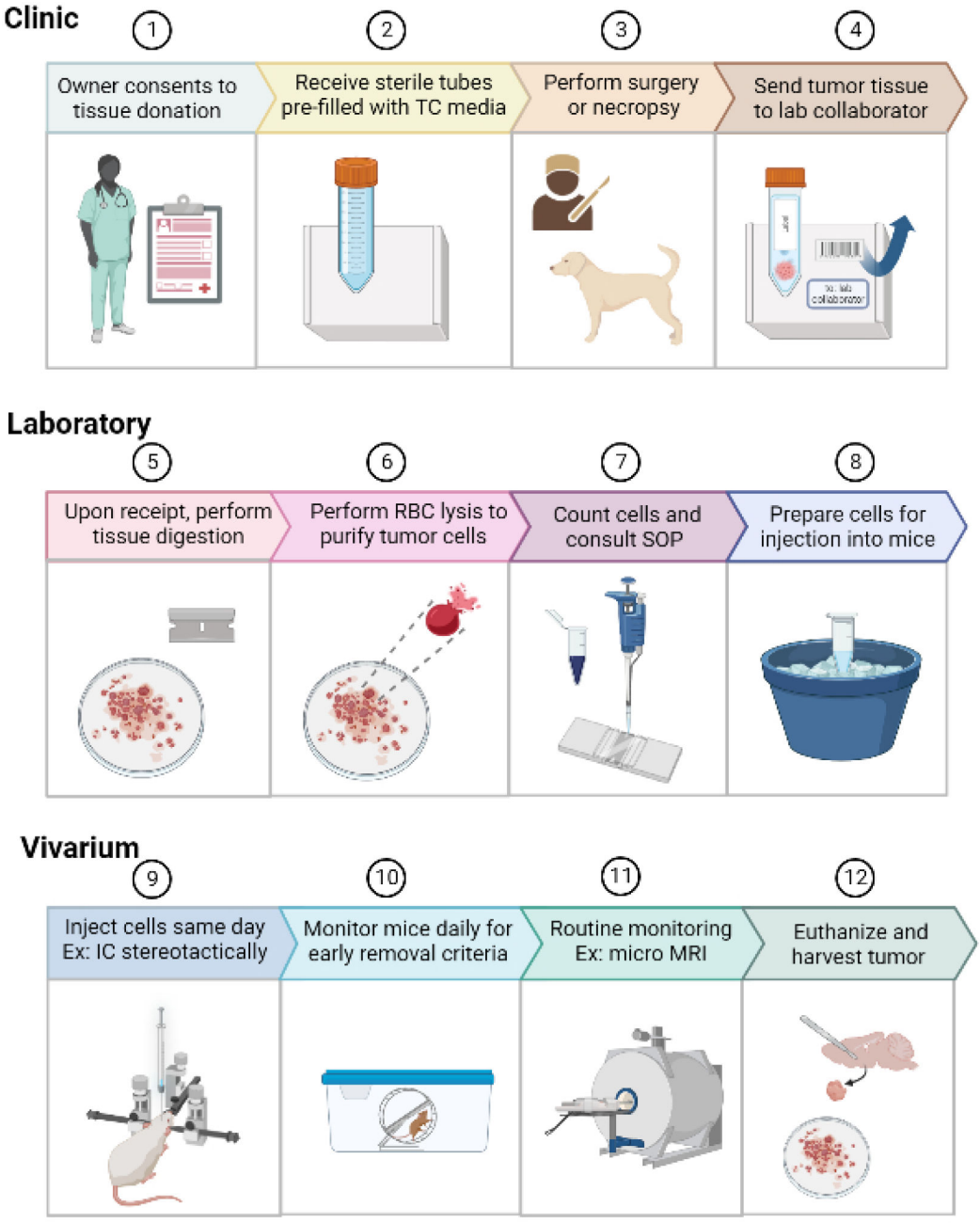

Figure 1. Schematic of workflow.

Establishing novel canine glioma patient-derived lines requires clinical, laboratory, and lab animal expertise. 1) Veterinary oncologist or pathologist requests consent for tumor tissue donation during surgery or immediately after necropsy. 2) Laboratory collaborator sends sterile tubes pre-filled with tissue culture media to clinician overnight on ice. 3) Clinician harvests tumor tissue at surgery or necropsy. 4) Tumor tissue is placed in tubes with tissue culture media and shipped overnight on ice back to laboratory collaborator. 5, 6) Upon receipt in the laboratory, tissue is processed with a papain digestion, followed by red blood cell (RBC) lysis. 7) Tumor cells are counted with a hemocytometer and the standard

operating protocol (Figure 2a) is followed based on the total cell number. 8) Cells are prepared for intracranial (IC) or subcutaneous (SC) injection. 9) Immunocompromised mice are injected IC or SC the same day as tissue processing. 10) Mice are monitored daily for signs of tumor growth, including weekly measurement with calipers for SC tumors. 11) Mice injected IC undergo microMRI imaging to monitor tumor size. 12) Upon signs of early removal criteria, mice are sacrificed, tumor tissue is harvested, and processed as in 5 and 6 above.

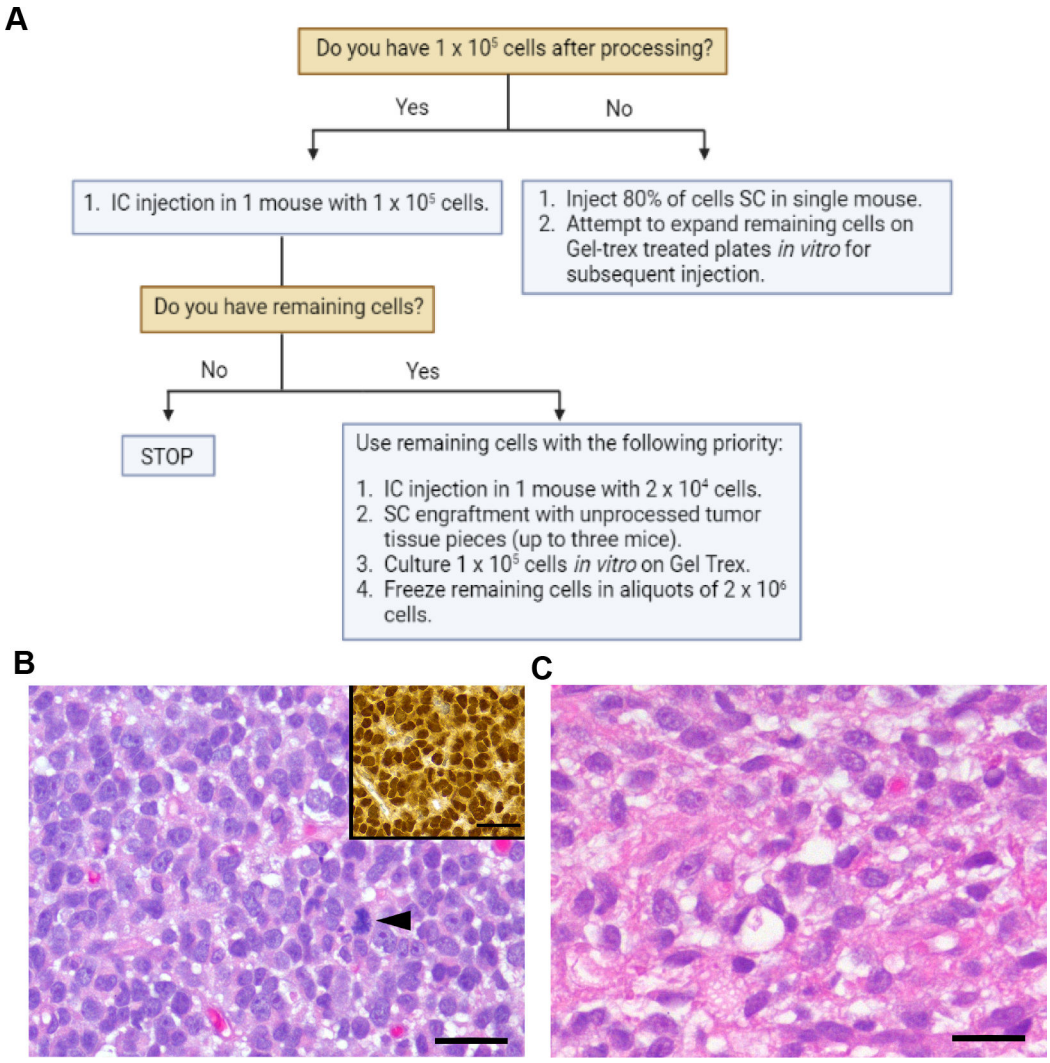

Figure 2. Acquisition and processing of cHGG cells.

A) Standard operating protocol for deciding priority of injections based on cell number upon receipt and processing (papain digestion and red blood cell lysis) in the laboratory. **B,C)** Photomicrograph of high-grade oligodendroglioma in a Boxer dog from which the Mo-HO patient-derived line was established. **B)** Note large nuclei, multiple nucleoli, and a mitotic figure (arrowhead). HE stain. Bar = 25 μm. Inset: Nuclei of the neoplastic cells express Olig2. Immunohistochemistry with diaminobenzidine chromogen and hematoxylin counterstain. Bar = 25 μm. **C** Note "fried egg" appearance of the neoplastic cells with their perinuclear clearing and artifactually accentuated cell borders. HE stain. Bar = 25 μm.

A

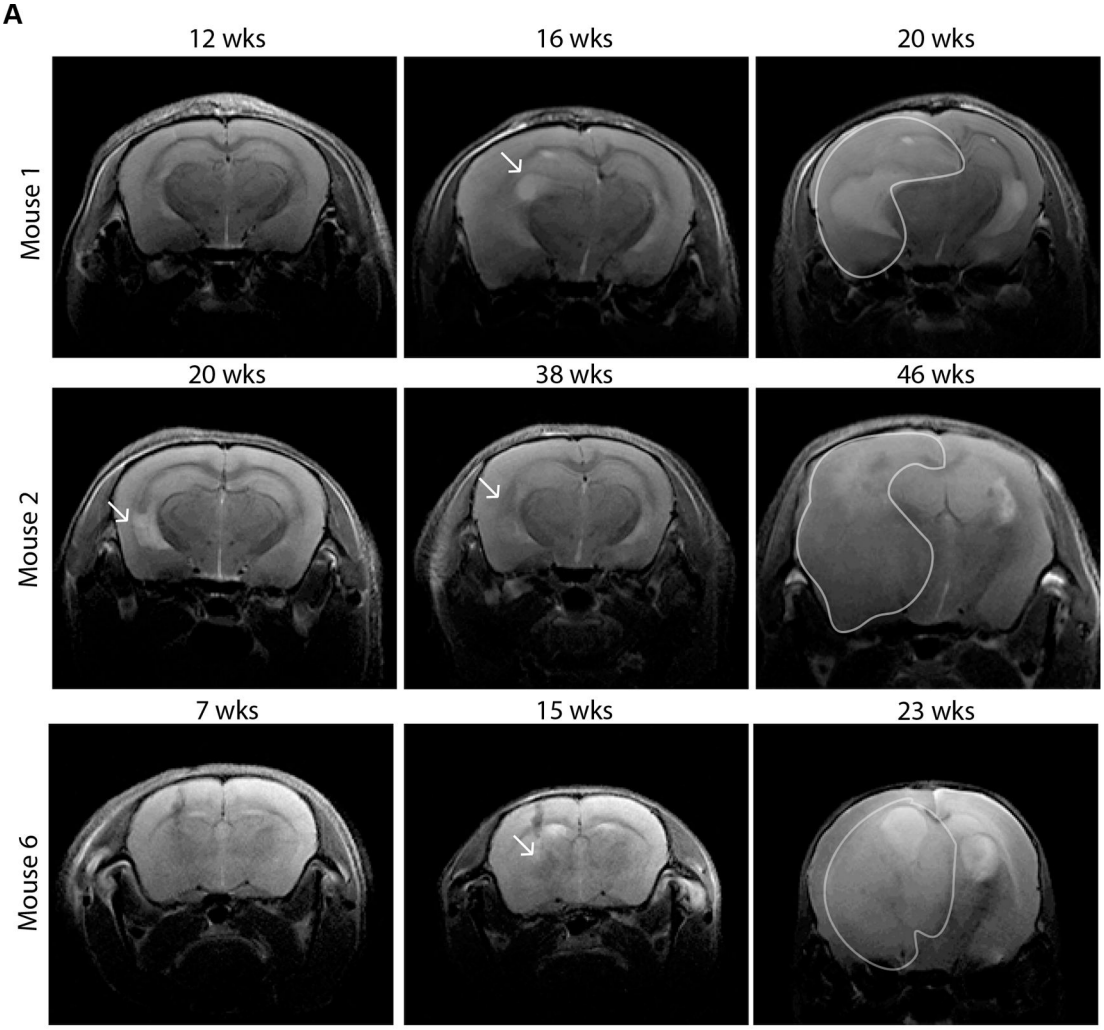

B

Mouse #	Cells	Cell # injected	Route	First sign of tumor	Sacrifice
1	Mo-HO	100,000	IC	16 wks	21 wks
2	Mo-HO	20,000	IC	38 wks	48 wks
3	Mo-HO	tissue	SC	12 wks	25 wks
4	Mo-HO	tissue	SC	22 wks	46 wks
5	Mo-HO	tissue	SC	-	46 wks
6	Boo-HA	100,000	IC	15 wks	23 wks
7	Boo-HA	20,000	IC	23 wks	25 wks

Figure 3. Monitoring cHGG cells in laboratory mice.

A) Transverse slices from T2-weighted microMRI imaging of mice engrafted with cHGG cells intracranially. The arrow in Mouse 2 at 20 weeks denotes a hyperintense signal which corresponds to edema or tumor growth. Other white arrows indicate tumor growth as hyperintense or hypointense regions. Outlines demonstrate tumor tissue edges. **B)** Chart denoting cHGG growth outcomes of mice injected IC or SC with Mo-HO and Boo-HA cHGG cells.

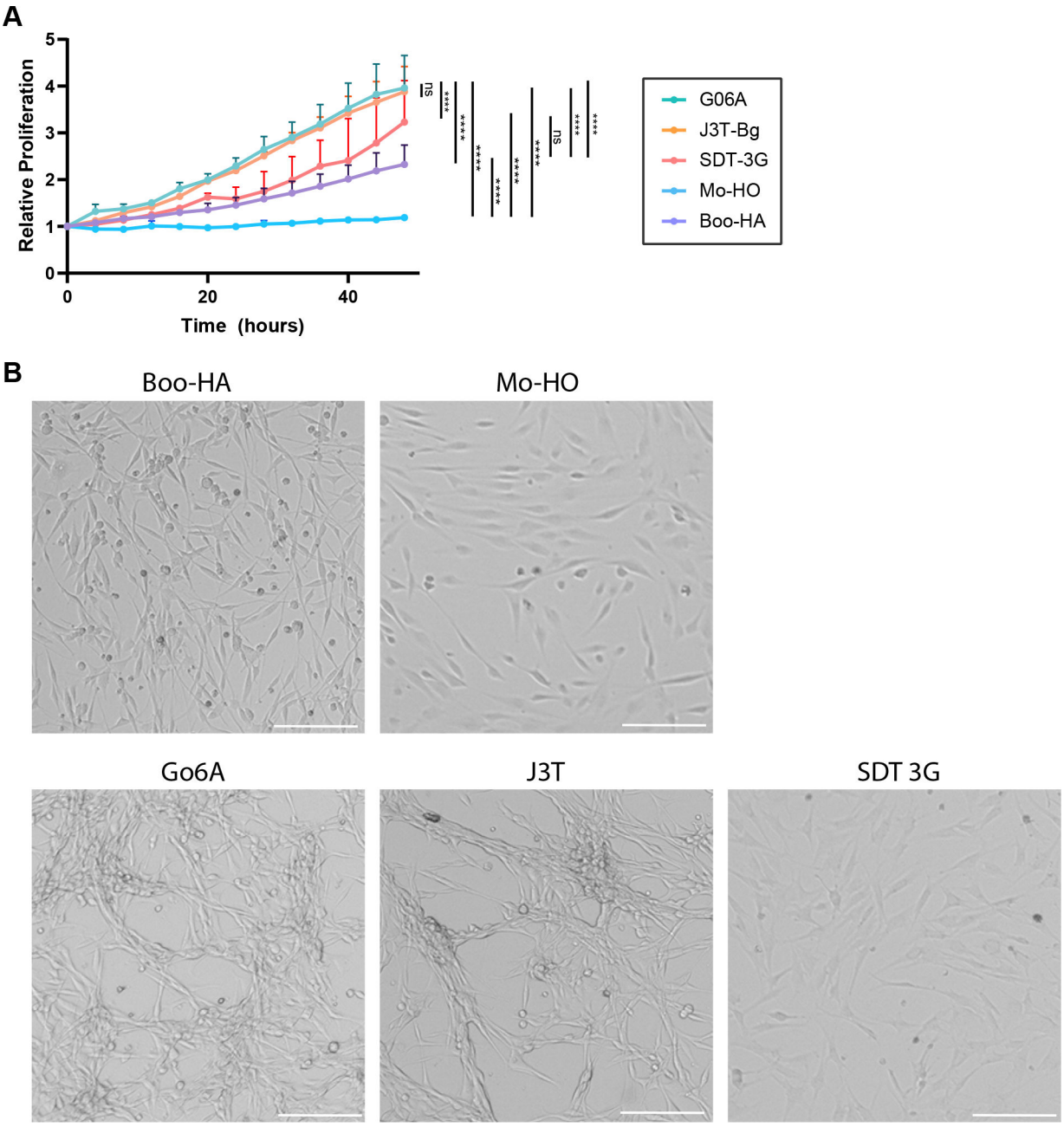

Figure 4. Morphology and proliferation of cHGG patient-derived and traditionally established cell lines.

A) Bar graph depicting growth of cells quantified as relative proliferation. Growth was monitored via IncuCyte ZOOM live-cell imaging system and percent confluence was quantified with a processing definition which created a mask overlay over cells. Each experiment was repeated three times per cell line with three technical replicates. Error bars depict standard error; ns, no significance; ****, $p < 0.0001$. **B)** Photomicrographs depicting morphology of corresponding canine HGG patient-derived or traditionally established cell lines. Scale bar = 150 μm.

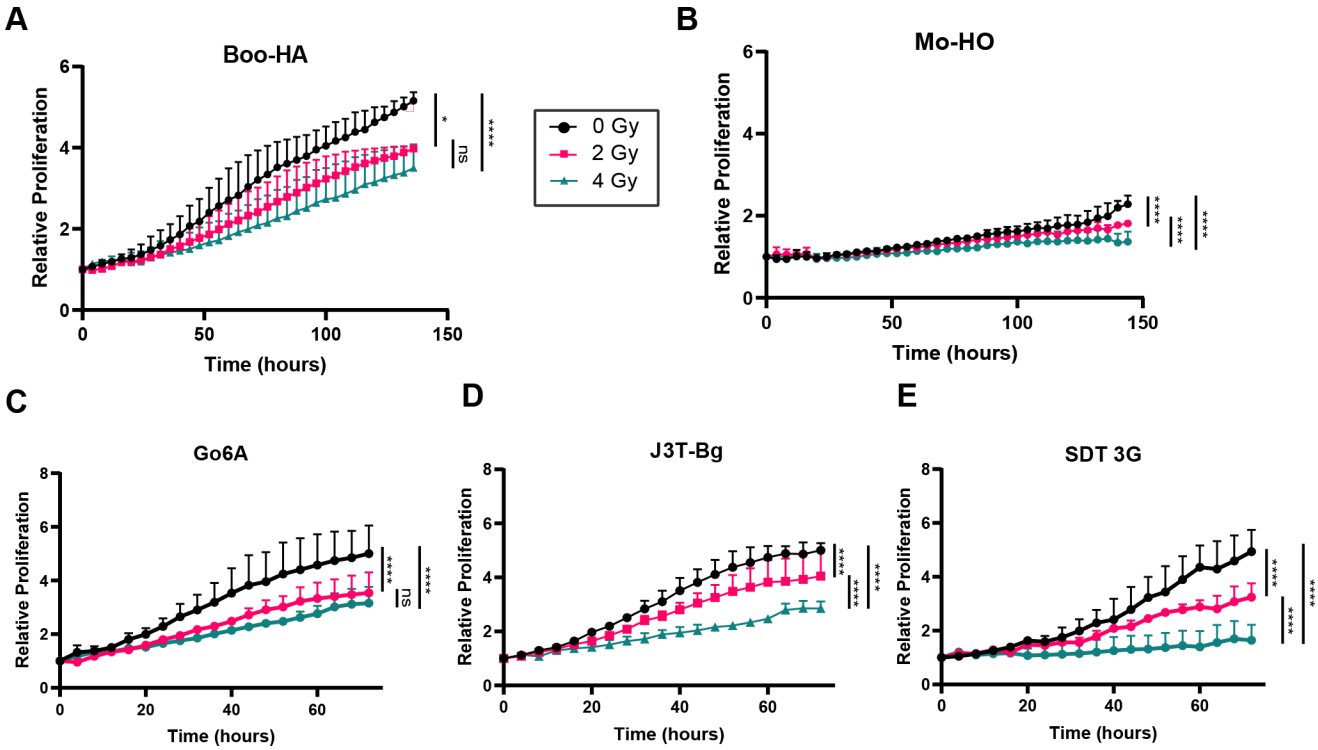

Figure 5. Short-term sensitivity of canine glioma cells to radiation.

Graphs depicting relative proliferation of corresponding cHGG lines Boo-HA **(A)**, Mo-HO **(B)**, Go6A **(C)**, J3T-BG **(D)**, and SDT 3G **(E)** when exposed to 0, 2, or 4 Gy radiation. Growth was monitored via IncuCyte ZOOM live-cell imaging system and percent confluence was quantified with a processing definition which created a mask over cells. Error bars depict standard error; ns, no significance; *, $p < 0.05$; ****, $p < 0.0001$. Each experiment was repeated three times per cell line with three technical replicates.

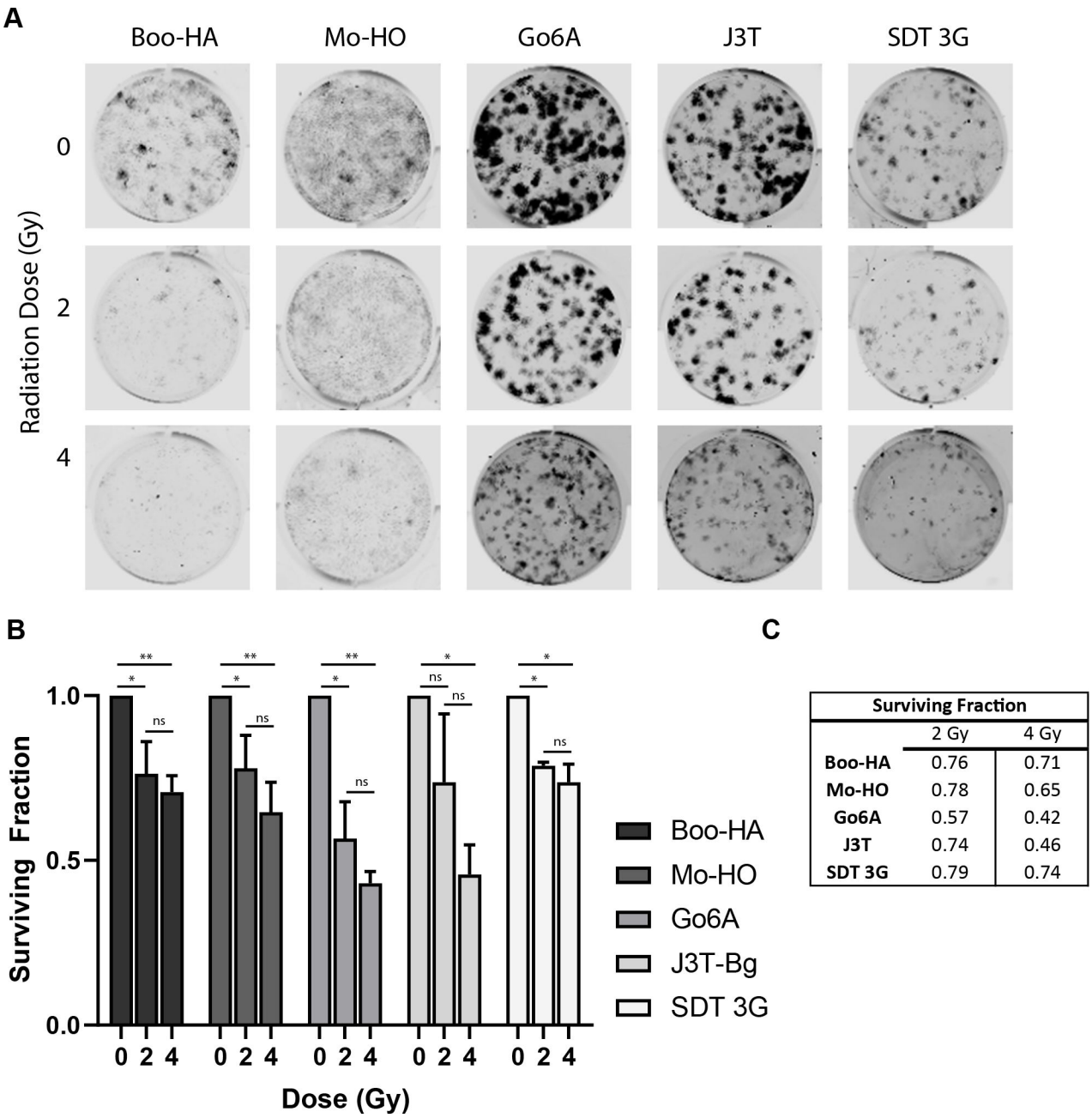

Surviving Fraction	2 Gy	4 Gy
Boo-HA	0.76	0.71
Mo-HO	0.78	0.65
Go6A	0.57	0.42
J3T	0.74	0.46
SDT 3G	0.79	0.74

Figure 6. Long-term sensitivity of canine glioma cells to radiation.

A) Representative images of long-term growth assays of cHGG cell lines following exposure to radiation. **B)** Graph depicting surviving fraction from A quantified as intensity and normalized to 0 Gy. Each experiment was repeated three times with three technical replicates per repeat. Error bars depict standard of error; ns, no significance; *, $p < 0.05$; ***, $p < 0.001$. **C)** Chart depicting mean surviving fraction from A.

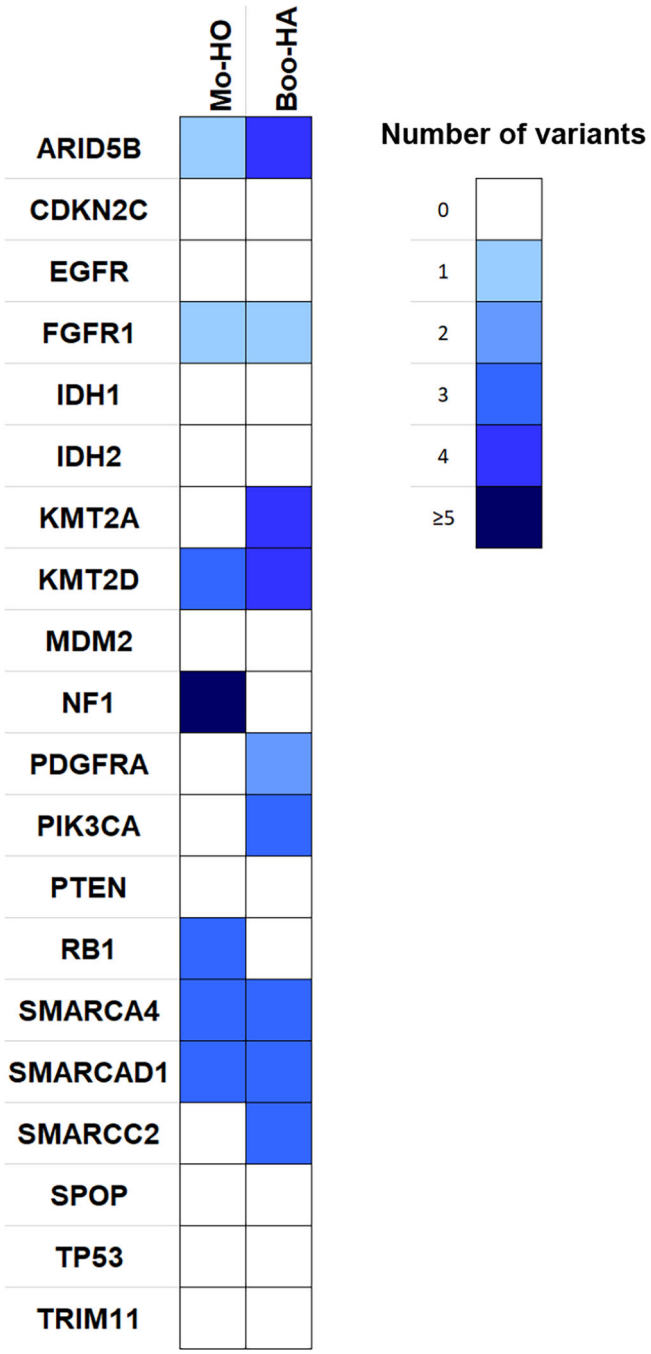

Figure 7. Variant analysis for novel cHGG patient-derived lines.

Heatmap indicating number of low impact variants (synonymous or located in a splice region) within 25 commonly altered genes in cHGG for novel patient-derived lines, Boo-HA and Mo-HO.